

DOI: 10.1002/ ((please add manuscript number))

## Full Paper (Advanced Materials Technologies)

# Porous PDMS-based Microsystem (ExoSponge) for Rapid Cost-effective Tumor Extracellular Vesicle Isolation and Mass Spectrometry-based Metabolic Biomarker Screening

Joseph Marvar<sup>1,+</sup>, Abha Kumari<sup>1,+</sup>, Nna-Emeka Onukwughu<sup>1</sup>, Abhinav Achreja<sup>2</sup>, Noah Meurs<sup>2</sup>, Olamide Animasahun<sup>2</sup>, Jyotirmoy Roy<sup>2</sup>, Miya Paserba<sup>2</sup>, Kruthi Srinivasa Raju<sup>1</sup>, Shawn Fortna<sup>3</sup>, Nithya Rammath<sup>4</sup>, Deepak Nagrath<sup>1,2</sup>, Yoon-Tae Kang<sup>1,\*</sup>, and Sunitha Nagrath<sup>1,5\*</sup>

<sup>1</sup>Department of Chemical Engineering and Biointerfaces Institute, University of Michigan, 2800 Plymouth Road, NCRC B10-A184, Ann Arbor, MI 48109, USA

<sup>2</sup>Department of Biomedical Engineering, University of Michigan, Ann Arbor, MI, USA

<sup>3</sup>Department of Mechanical Engineering, University of Michigan, G.G. Brown Laboratory, 2350 Hayward, Ann Arbor MI 48109

<sup>4</sup>Department of Internal Medicine, University of Michigan, Ann Arbor, MI, 48109 USA

<sup>5</sup>Rogel Cancer Center, University of Michigan, 1500 E Medical Center Dr. Ann Arbor, 48109

\*Correspondence: Dr. Sunitha Nagrath ([snagrath@umich.edu](mailto:snagrath@umich.edu)) and Dr. Yoon-Tae Kang ([kyoontae@umich.edu](mailto:kyoontae@umich.edu))

**Keywords:** Porous PDMS, microsystems, circulating biomarkers, PDMS Sponge, extracellular vesicles, liquid biopsy

## Abstract

Polydimethylsiloxane (PDMS) is inexpensive robust polymer that is commonly used as the fundamental fabrication material for soft-lithography based microfluidic devices. Owing to its versatile material properties, there are some attempts to use PDMS as a porous 3-D structure for sensing. However, reliable and easy-fabrication has been challenging along with the inherent hydrophobic nature of PDMS hindering its use in biomedical sensing applications. Here, we report a cleanroom-free inexpensive method to create 3-D porous PDMS structures, “ExoSponge” and its effective surface modification to functionalize its 3-D porous structure. We demonstrate the ability of ExoSponge to recover cancer-associated extracellular vesicles (EVs) from complex biological samples of up to 10 mL in volume. When compared to ultracentrifugation, the ExoSponge showed a significant increase in cancer EV isolation of more than 210%. We further employed targeted ultra-high pressure liquid chromatography-tandem mass spectrometry to profile 70 metabolites in the EVs recovered from the lung cancer patient’s plasma. The resulting profiles revealed the potential

This is the author manuscript accepted for publication and has undergone full peer review but has not been through the copyediting, typesetting, pagination and proofreading process, which may lead to differences between this version and the [Version of Record](#). Please cite this article as [doi: 10.1002/admt.202201937](https://doi.org/10.1002/admt.202201937).

This article is protected by copyright. All rights reserved.

intraexosomal metabolite biomarker, phenylacetylglutamine (PAG), in non-small cell lung cancer. The high sensitivity, simple to use and cost-effectiveness of the ExoSponge platform creates huge potential for rapid, economical and yet specific isolation of exosomes enabling future diagnostic applications of EVs in cancers.

## Introduction

Extracellular vesicles (EVs) are naturally secreted membrane bound nanovesicles from cells that are involved in intercellular communication. Their membrane contains and protects proteins, nucleic acids, and metabolites. Hence, they can serve as active cargo delivery vehicles and messengers of genetic information [1]. There has been an increased interest in the clinical use of EVs as biomarkers due to their significance in cellular signaling, disease progression, and therapeutics. The isolation and characterization of exosomes enable the ability to use them as reliable biomarkers for minimally invasive disease diagnosis, called liquid biopsy. One of the promising opportunities for disease diagnosis is cancer diagnosis, since EV secretion is increased by many cancer types. Their presence in a variety of biosamples – i.e., blood, urine, saliva – makes them an attractive avenue for exploration for liquid biopsy to provide a simple, *in vitro* analysis of a patients' tumor status [2, 3]. Deregulated cellular metabolism has been established as a hallmark of cancer which supports the use of metabolite characterization as a sensitive, inexpensive, origin-agnostic tool for minimally-invasive diagnosis of cancer [4]. However, the large amounts of biosample contaminants and the size of the desired endosome-derived small EVs (sEV), also called exosomes, at just 30-150 nm diameter makes isolation difficult and challenging [5] using conventional EV isolation methods.

Ultracentrifugation (UC) is the primary practice used for EV isolation being considered the “gold standard”. However, UC requires expensive machinery, large operating dilution ratios, and a long procedure time which makes small or mid-bulk volume (100µl-5ml) sample isolation impractical. Other techniques such as the use of magnetic bead kits and

polyethylene glycol (PEG) have been effective with minimal volume samples but magnetic bead kits can only accommodate low sample throughput and PEG has low EV specificity due to its principle of settling all small-sized particles during processing. Even when only obtaining low purity yields, a bulk sample of just several milliliters would be too expensive for PEG, with prices of \$100 per test when scaling up [6]. Recent works using methacrylate-based monolithic disc columns utilize selective immunoaffinity-based isolation of platelet-derived EVs from plasma [7,8]. However, poor yields and the inability to isolate a specific subpopulation of EVs limit their applications in downstream analysis for clinical studies.

Microfluidic approaches have shown superior specificity and high-throughput performance for samples up to sub milliliter in volume [9-11], however, it is not cost effective when it comes to processing mid-bulk volume samples (1-10ml), which is often needed for genomics/metabolomics studies with enough sample quantities to be detected. Their bulk isolation ability is limited by their total sample processing volume per device that usually handle sub-microliter samples. Thus, technologies that can isolate EVs from mid-bulk samples at lower costs and high yields are urgently needed. Some recent attempts towards this topic include ExoTic, a size-based isolation chip that produces high yield and purity of isolated EVs from low to high volumes of samples [12]. However, it can be limited by filter clogging issues as well as pump stalling with flow rates higher than 5ml per hour for small pore size filters. Additionally, our group recently devised a liquid biopsy hydrogel platform, ExoBeads, for easily scaling up antibody-based EV isolation for larger volume samples [13]. Here, we present our new PDMS-based quick EV isolation platform, ExoSponge, which is cheaper and has easier sample handling when compared to ExoBeads.

Polydimethylsiloxane (PDMS) is commonly used to fabricate cheap, robust, and high-resolution microfluidic systems in the fields of biology and medicine such as microfluidic

devices, microreactors, and micro channels for electrophoresis [14, 15]. There have also been attempts to utilize PDMS's versatile properties to construct porous 3-D structures, such as the porous microneedles developed by Takeuchi et al. for non-invasive healthcare monitoring [16]. However, previous studies describe diverse application of the PDMS structures ranging from pressure sensing to the use in protective layers for robotics [17-20]. Furthermore, the inherent hydrophobic nature of PDMS makes the manipulation of elements in aqueous solutions ineffective and impractical such that there have not been attempts combining PDMS porous 3-D structure with its biocompatible potential. As a result, previous works discussed various fabrication technologies for 3-D porous PDMS platforms but with limited biological applications [21, 22]. Here, we present a unique yet simple fabrication method to create the 3-D porous PDMS sponge-like structure. Our method uses simple sugar cubes for creating the porous structures and does not require any cleanroom processing to create the bio-functional 3-D porous structure. We describe a chemical treatment approach that oxidizes its large surface area making it optimal for its use with bio samples.

Utilizing the hydrophilicity of oxidized PDMS along with the high surface area characteristics of the porous 3-D structure, we can create a suitable scaffolding for immuno/lipid-affinity based biomarker isolation, such as EVs. With additional functionalization and target-capturing molecule conjugation, our porous PDMS platform, ExoSponge, can selectively target exosomes to isolate them from bulk samples of up to 5-10mL (**Fig.1**). Previously, a highly sensitive method of isolation of exosomes with a limit of detection of  $2.9 \times 10^8$  exosomes/ml was achieved using an anti-CD63 based immunoassay [23]. Similarly, Annexin V-based lipidaffinity-based capture demonstrated the specific isolation of cancer-associated exosomes with an average capture efficiency of 90% [24]. Thus, our devices were conjugated with anti-CD63 antibodies to target the tetraspanin CD63

on exosomes and Annexin V for the specific capture of cancer-associated exosomes, respectively. To demonstrate the efficacy of this device, exosomes were isolated from serum samples of healthy and lung cancer patients using ExoSponge. The exosomes were further analyzed by liquid chromatography tandem mass spectrometry (LC-MS/MS) followed by untargeted metabolomics to quantitatively profile the metabolite cargo of lung cancer exosomes. Previous EV isolation methods exacerbate the challenge of extracting metabolites at concentrations large enough to profile a broad range of polar metabolites. In addition, polar metabolite analysis from exosomes required over  $5 \times 10^{10}$  exosomes, obtainable from a culture of  $15 \times 10^6$  cells over 48 hours [25,26]. While blood has a much higher concentration of exosomes at  $10^{10}$ - $10^{12}$ /mL, ultracentrifugation and solvent precipitation-based isolation techniques would still require at least 2-10 mL of blood plasma to provide an equivalent yield to that of ExoSponge [27]. Moreover, the ability to isolate and extract metabolites on the ExoSponge minimizes the metabolite degradation and loss due to residual enzymatic activity and long procedures throughout the ultracentrifugation isolation and extraction steps.

Thus far, metabolic profiling of exosomes has been performed after extraction via ultracentrifugation or precipitation assays [26, 28-29] and largely focused on lipidomics [30-32]. To the best of our knowledge, this is the first demonstration of a comprehensive study of small-molecule polar metabolites using a PDMS-based microsystem and our innovative porous PDMS scaffolding for affinity-based isolation can provide rapid, high-yield, and inexpensive EV isolation and profiling solution. These metabolites can be used to profile the metabolic state of the secreting cells through their soluble contents, providing an indication of the activity levels of a broad array of metabolic pathways. Due to the potent and diverse metabolic reprogramming of cancers, alterations in levels of polar metabolites contained within exosomes can serve as a simple, noninvasive readout for cancer diagnosis. Our results

highlight the advantages of how the ExoSponge and the SCIEX 7500 UPLC-MS/MS can be uniquely integrated to overcome the challenges of broad metabolic profiling of extracellular vesicles.

## Results and discussion

**Cleanroom-free fabrication of porous 3-D PDMS sponges.** We have utilized commercially available widely used sugar cubes as a scaffold to make the porous PDMS sponges (**Fig.2a**). The sugar cubes were coated with a 10:1 PDMS pre-polymer and curing agent, then placed into a vacuum chamber for 40 minutes and subsequently placed in a 68°C convection oven overnight for curing. To dissolve the sugar scaffold, the PDMS coated sugar cubes were carefully cut out from their container and submerged into a beaker of 90°C water for 1-2 hours with constant stirring. The beakers were replaced with fresh water every 30 minutes to maximize sugar transport. Lastly, the PDMS-sugar cube devices were stored in a 70% ethanol beaker overnight and squeezed dry of excess ethanol upon functionalization.

**Characterization of Porous PDMS** The porous PDMS structure creates a high-surface area device with an ability to be easily modified for functionalization (**Fig. 2b**). The device inherits the micro-pores of the sugar scaffolding. Analysis of cross-sectional slices of the device showed the pore sizes are semi-consistent throughout with an average pore diameter of  $408.9 \mu\text{m} \pm 91.8$  as shown in **Figure 3a**. The pore size-frequency follows a normal distribution (**Fig.3a right**). Also, the center slice diameters tend to be the largest with the pore sizes decreasing toward the surface of the device. This could be a result of the PDMS resin not being able to penetrate as effectively into the sugar cube's center as it would on the

surface. The cross-sectional view of porous PDMS cut is shown in **Figure 3b**. We further evaluated the compressibility/wettability of the ExoSponge which allows the device to release absorbed liquid such as biological samples (**Fig. 3c**). After oxidation by piranha solution treatment, the device is transformed from the inherent hydrophobicity of PDMS to be hydrophilic. This not only increases the wettability of the device for aqueous solutions but also roughens the surface of the device for higher binding chance between device and EVs [33,34].

The porosities of the unfunctionalized device ( $72.7\% \pm 5.08\%$ ) and sugar cube scaffolding used ( $34.2\% \pm 1.14\%$ ) were measured along with the device after functionalization ( $57.9\% \pm 2.21\%$ ) (**Fig. 3d**). Following silane-GMBS and NeutrAvidin conjugation, the devices were evaluated with biotinylated fluorescent dye to check whether the device was effectively conjugated with avidin. The results in **Figure 3e** show the avidin conjugation was successful yielding fluorescence intensities more than 7x the unmodified control porous PDMS.

**Demonstration of EV isolation using EV capturing molecule conjugation** The Annexin V conjugation on the device will selectively bind to phosphatidylserine on cancer-derived extracellular vesicles in the presence of calcium ions while an anti-CD63 conjugated device will isolate general CD63 tetraspanin protein-expressing EVs that is common for exosome isolation (**Fig. 4a**). This versatility will allow the ExoSponge device to isolate general EVs or specific subpopulations on demand in a sample based on the experiments. In **Figure 4b**, the SEM images show the capture of exosomes on the Annexin V-conjugated porous device's surface. Further, the Annexin V-conjugated device will eventually be subjected to an EDTA solution that will remove the calcium ions, disrupt the affinity, and release the isolated EVs.

**EV isolation/release performance using ExoSponge** The ExoSponge has been optimized concerning EV capturing molecules, optimal incubation time, device size, and external force during isolation. The optimization was evaluated in terms of total EV concentration, exosome-sized concentration, and purity of the samples. Exosome concentration was calculated from EVs in the size range of 30-150 nm and purity was determined as the fraction of isolated EVs that were exosomes. We first compared the EV capturing performance between Annexin V(Av) conjugated ExoSponge and anti-CD63 conjugated ExoSponge (**Fig. 4c**). While anti-CD63 is a widely used exosome markers in immunoaffinity-based capture, the Av-conjugated ExoSponge captures 30% more lung cancer cell-derived exosomes (H3255) than anti-CD63-conjugated ExoSponge, which demonstrates cancer-associated EV isolation of Av-conjugated ExoSponge. The SEM images of ExoSponge with various EV capturing molecules showed the similar results (**Figure S1**)

The incubation time of ExoSponge with the sample was also optimized. After incubation trials of 20-, 40-, and 60-minute periods, the exosome concentrations and total EV concentrations were recorded (**Fig. 4d**). The results demonstrate a positive correlation between increased incubation time and increased exosome concentration. However, the 40-minute period was determined optimal due to diminishing marginal gains as the incubation got longer. This allows for significant EV isolation while keeping the procedure time minimal.

The high surface area of the ExoSponge device might be responsible for its effective EV isolation. To analyze the effect of any further increase in surface area, the sugar cube template size was cut to decrease the volume to one-eighth of the original. The isolated sample's exosomal concentration and its purity were measured for both the original and



smaller cube sizes, with total device volume constant for each trial. In **Figure 4e**, it shows the eight smaller cubes outperformed the original with an exosome concentration of  $1.86 \times 10^9$  EVs/mL while the original cube only produced  $8.36 \times 10^8$  EVs/mL. In addition, the purity also increased from 56.5% to 65.3% for the smaller cubes. However, the increased surface area of the smaller devices makes the total adsorbed volume increase from 1.9 mL per cube to 2.6 mL for the smaller cubes. This makes the EV concentrations similar regardless of device size. For this reason and that the smaller cubes make manipulation more difficult, the standard sugar cube size was chosen.

In attempts to reach higher isolation concentrations, the cubes were subjected to additional mechanical agitation from centrifugation (1000 rpm for 10 min) during incubation. For this optimization experiment, the devices were separated with half being subjected to centrifugation during its incubation while the rest were kept on a rocker. In **Figure S2**, the presence of the external centrifugal force had no significant effect on the EV isolation concentration. The rocker incubation method was selected to keep the procedure simple.

**EV recovery comparison study** The ExoSponge device's isolation was compared to the gold-standard isolation method, ultracentrifugation (UC), as well as a porous PDMS device without capturing molecule conjugation. Using NTA analysis, the ExoSponge device outperformed both methods in the total number of isolated EVs and its resulting sample exosome concentration when conjugated with anti-CD63 and Annexin V (**Fig. 4f, Fig S3**). Even with the higher measured exosome concentration, the ExoSponge device has no significant drop in the isolated sample purity when compared to UC. **Figure 4g** shows UC with mean sample purity at  $76.5 \pm 17.7\%$  and ExoSponge sample resulting in a purity of  $90.9 \pm 1.83\%$  when functionalized with Annexin V, which shows greater exosome specificity

using the ExoSponge device. This is as expected and proves the reliability of our porous PDMS platform regardless of the choice of antibody used for isolation. Additionally, in **Figure 4h**, micro-BCA protein analysis of the isolated exosomes also demonstrates ExoSponge as the more effective bulk isolation method when compared to UC. Western blot analysis of the recovered exosomes profiled proteins commonly found in cancer-derived EVs. These results show the ExoSponge device is a significantly more effective isolation method for bulk samples even when compared to the previous gold standard procedure.

**Exosome isolation from plasma samples collected from lung cancer patients** After analysis of the cell culture supernatant, we validated our device to study clinical specimens using patient plasma samples. We collected a plasma sample volume of 10 mL and used ExoSponge to isolate EVs as described in experimental section. Subsequent to capture of the EVs, they are released from the ExoSponge and analyzed by NTA. NTA analysis displayed successful EV isolation from both healthy and lung cancer samples and the ExoSponge device continued to outperform UC (**Fig. 5a**) as well as more exosome-sized vesicle distribution (**Fig. 5b**) For the lung cancer patient samples, ExoSponge yielded an average exosome isolation of  $9.40 \times 10^9$  EV/mL while only  $3.26 \times 10^9$  EV/mL for UC. In the healthy donor sample, ExoSponge and UC resulted in  $2.64 \times 10^9$  EV/mL and  $2.23 \times 10^9$  EV/mL, respectively (**Fig. 5a-left**). The smaller isolation difference in healthy donor cells could be a result of healthy cells not expressing much phosphatidylserine (PS) in comparison to cancer cells. We further quantified the total protein of the EVs isolated using both methods. As shown in **Figure 5a-right**, BCA analysis draws the same conclusion with ExoSponge having a protein quantity of  $732.3 \pm 10.6$   $\mu$ g/mL and UC with only  $81.1 \pm 34.0$   $\mu$ g/mL. The purity of the NTA isolated exosome sample was evaluated by the ratio of EV

sized over all particles measured in solution. This analysis indicates that, unlike UC, ExoSponge has a higher purity for its cancer patient samples when compared to the healthy.

The surface of the functionalized ExoSponge device was mapped using a SEM after biosample exposure but before it was subjected to EDTA treatment to release exosomes. The SEM images show the porous 3-D structure of the device and as the magnification was increased, EV-sized clusters (30-150  $\mu\text{m}$ ) appeared on the surface of the device providing visual evidence for successful exosome capture (**Fig. 5c**). The resultant from 4 different clinical samples showed housekeeping protein, GAPDH, and exosomal marker CD63 expression (**Fig. 5d**).

Further analysis of more blood plasma samples showed preferential isolation of exosomes derived from cancer patients in comparison to healthy ones (**Fig. 5e**). ExoSponge yielded a mean exosome isolation concentration of  $2.46 * 10^9 \pm 7.31 * 10^8$  EVs/mL for the healthy donor samples and  $6.36 * 10^9 \pm 5.03 * 10^9$  EVs/mL for the lung cancer patients (**Fig. 5f**). Previous research has highlighted the possible preference of Annexin V for cancer-derived EVs which may explain the higher isolation for the cancer patient samples [24]. This high recovery of exosomal EVs demonstrates the efficacy of ExoSponge in isolating EVs of interest for clinical use.

**Exosomal metabolites analysis using mass spectrometry** The utility of serum and urinary metabolites as biomarkers for diseases has been well-established. More recently, with the discovery of metabolic cargo in exosomes [26], the potential of exosomal metabolomics for discovering biomarkers has been more broadly recognized. Metabolomics profiling of intraexosomal cargo can prove to be a strong reflection of intratumoral metabolism that is

unaffected by systemic metabolism and circulating metabolites. In this study, to this end, we extracted intraexosomal metabolites directly from exosomes adsorbed on the ExoSponge conjugated with Annexin V and anti-CD63. The high yield efficiency of the ExoSponge and in situ extraction of metabolites from captured exosomes, coupled with the highly sensitive SCIEX 7500 UPLC-MS/MS allowed detection of metabolites in exosomes isolated less than 1 mL of blood plasma. Moreover, the ability to isolate and extract metabolites on the ExoSponge minimized the metabolite degradation and loss due to residual enzymatic activity and long procedures throughout the ultracentrifugation isolation and extraction steps.

The metabolite extracts were then profiled for polar metabolites using an LC-MS/MS workflow that covers over 500 MRMs corresponding to approximately 400 unique compounds. After performing requisite quality checks (Methods), from a data set using ExoSponge conjugated with Annexin V, we detected 90 MRMs corresponding to 68 metabolites across the sample set, demonstrating an overall distinct profile of exosomal cargo in lung cancer patients compared to healthy subjects (**Fig. 6a**). From a data set using ExoSponge conjugated with anti-CD63, there were intra-group variations between cancer and healthy groups and they were not statistically significant. One-factor statistical analysis revealed that 36 of 68 metabolites extracted from ExoSponge (Av) displayed large differences (fold-change  $>2$  or  $<2^{-1}$ ) in intraexosomal levels in lung cancer-derived exosomes compared to exosomes in healthy subjects (**Fig. 6b**). However, only one metabolite, phenylacetylglutamine (PAG) was statistically significantly higher in lung cancer-derived exosomes compared to healthy controls (**Fig. 6c**). This indicates that intraexosomal PAG level is a potential biomarker for lung cancer. High levels of PAG are found in urine of patients with disruption in nitrogen metabolism due to hyperammonemia, urea cycle disorders, cardiovascular disease and cancer [35-38]. PAG is synthesized in the

liver and filtered out through kidneys as a mechanism of ammonia clearance, but also produced by the gut microbiome [37, 39]. Interestingly, metabolite set enrichment analysis (MSEA) in reference to metabolic signatures of diseases available in MetaboAnalyst (Methods), revealed enrichment of biomarkers for phenylketonuria, cachexia in cancer patients, methylmalonic aciduria (**Fig. 6d, 6e**, Supplementary Table S2). Interestingly, we observed levels of betaine and choline trended higher in cancer-derived exosomes (**Fig. 6f**), which along with PAG have been described as biomarkers for prostate cancer risk [38]. Further, we also noticed remarkably high levels of methylmalonate (MMA) in two of the cancer-derived exosome samples (**Fig. 6g**). Interestingly, age-related accumulation of intracellular MMA has been found to be a mediator for tumor progression through SOX4 [40]. The capture of exosomes and extraction of intraexosomal metabolites with the ExoSponge (AV) is a novel avenue for discovering tumorigenic biomarkers that reflect intratumoral metabolism. Despite the heterogeneity we see in the metabolic profile of cancer-derived exosomes, our data strongly indicates that their metabolic cargo is distinct to that of exosomes in healthy subjects.

## Conclusion

Due to the stability of their lipid bilayer, EVs have been emerging as viable biomarker in many diseases including cancer and neurodegenerative diseases. However, the research has been hampered by easy access to specific EV isolation methods than can handle wide ranges of volumes. We provide an inexpensive, easily fabricated PDMS device, ExoSponge. We demonstrated that we could further modify the micro pores and make the device bio-

functional for specific capture of exosomes. This efficient isolation and quick characterization analysis can lead to point-of-care cancer diagnoses. The ExoSponge device outperformed UC in total exosome isolation while maintaining purity for these bulk samples in both clinical and model samples. Annexin V-conjugated ExoSponge effectively isolated exosomes from healthy and cancer patients. The simplicity of fabrication, the rapid sampling ability, and the functionalization versatility of porous PDMS makes it a promising topic of further exploration in its application in exosome isolation as well as other medical and biological biomarker detection. Since ExoSponge inherits the adaptable conjugation properties of PDMS while adding more flexibility in target capturing molecules and a higher surface area, it could serve as an effective affinity-based platform for other biomolecule isolation from bulk solutions. Importantly, in addition to discovering metabolic biomarkers, intraexosomal cargo can reflect the metabolic reprogramming such as urea cycle disruption or upregulated propionate metabolism in the originating cancer cells, which demonstrates the potential value of ExoSponge (Av) as a tool for accessible, non-invasive cancer diagnostics.

## Methods

***Porous PDMS fabrication:*** To prepare the porous PDMS blocks, a sugar cube was utilized as the scaffolding material [41, 42]. First, 1.5 x 1.5 x 1.5 cm sized sugar cubes (Domino, United States) are placed in a destructible flat weigh boat. The PDMS pre-polymer and PDMS curing agent mix (10:1) was poured over the sugar cubes until the level of the resin is equal to that of cubes. To facilitate adsorption of the resin into the pores of the cubes, the sugar-PDMS container was placed into a vacuum chamber for 10 minutes. After more PDMS mixture was added to keep the resin level above the cube, the sugar-PDMS mixture was

returned to the vacuum chamber for another 40 minutes. Lastly, the sugar-PDMS mixture was placed in a 68 °C convection oven overnight to allow the devices to cure.

The cured sugar-PDMS composite was extracted from the container and the individual cubes were cut out, carefully making sure each side of the cubes have the sugar exposed. To dissolve the sugar from the composite, the cut-out sugar-PDMS cubes were placed in a beaker of water at 90 °C for 1-2 hour(s) with stir rods. The water was swapped out after 30 minutes to avoid the water from becoming saturated. To remove the remaining sugar, the cubes were placed in a beaker of 70% ethanol overnight. Lastly, the resulting cube-shaped devices were squeezed out to remove any absorbed liquid and placed into a storage container until functionalization.

The porosity was determined by first measuring the approximate volume using a ruler. Then by taking the mass of the device, its density was determined. The calculation used the known densities of air and PDMS to calculate the air mass fraction of the device.

***Porous PDMS surface modification:*** For the device surface modification, it was first subjected to a piranha solution that contains sulfuric acid and hydrogen peroxide (3:1) for ten minutes to transform the PDMS's natural hydrophobic and oleophobic properties into a more hydrophilic surface [43]. This oxidizing transformation allows for the adsorption of aqueous, biological samples such as plasma, urine, and saliva. While the bath allows for sufficient oxidation of the surface, it also roughened the surface of the device which increases the surface area without affecting its ability to be further functionalized [44, 45]. The surface was then conjugated following previous standard avidin-biotin chemistry [13, 24] with optimization. Briefly, PDMS cubes were immersed into silane solution and incubated for an

hour. The cubes were then immersed and washed with ethanol. Next, the cubes were immersed into a GMBS mixture and incubated for 30 minutes. After further washing with ethanol, the cubes were submerged into an NeutrAvidin solution in a conical tube and incubated overnight in a standard refrigerator. On the day of experiment, the cubes were defrosted and washed out with filtered PBS. The coverage of NeutrAvidin in our cubes was evaluated and confirmed using biotinylated staining dye. The PBS wash was followed by the conjugation of EV binding protein, Annexin V or anti-CD63. The cubes for experiments were soaked into biotinylated Annexin V solution (50  $\mu$ L Annexin V + 1 mL of 1 $\times$  binding buffer) or anti-CD63 (20  $\mu$ L Anti-CD63+ 1 mL PBS) and incubated 40 minutes.

***Cancer cell culture and exosome sample preparation:*** We used H3255 lung cancer cell culture supernatant throughout this study. Cell lines were cultured in Dulbecco's modified Eagle' Minimal Essential Media (DMEM, Life technologies, Inc.). Media was supplemented with 10% (v/v) exosome-depleted fetal bovine serum (System Bioscience, LLC) and 1% (v/v) penicillin–streptomycin (Invitrogen).

For the exosome model samples, a count of  $1\times 10^5$  cancer cells were incubated in exosome-depleted media for 1 day, then cell culture supernatant (CCS) was gently replaced from the cell plate. This CCS was followed by mild centrifugation for excess cell or bigger aggregation elimination, and then 1-3 ml of CCS was prepared for model sample studies.

The sample collection and experiments were approved by University of Michigan Institutional Review Board (IRB). Informed consent was obtained from all participants of this clinical study and non-small cell lung cancer blood samples were gathered after approval of the institutional review board at the University of Michigan (HUM00119934). Blood samples



were centrifuged at 1000xg for 10 minutes to isolate and extract plasma from the blood. The plasma extract was further diluted with 10x binding buffer (10:1) for exosome isolation.

***EV isolation/release using ExoSponge:*** For sample processing, 2 ExoSponge devices were used for 5 ml of sample containing plasma or model exosomes (2.5 ml per device). Samples were either prepared in the 1x of binding buffer containing 2.5 mM of CaCl<sub>2</sub> to be actively conjugated with Annexin V (Cat #: BD 556417, BD Biosciences, USA) or 1x PBS buffer solution for anti-CD63-based experiments (Cat #: 215030, Ancell Corporation, USA). Before exosome isolation occurs, a 10x Binding Buffer is added to the biological sample at a 10 to 1 respective ratio of sample to buffer. For cell supernatant samples, we incubated for 20 to 60 minutes. After incubation at room temperature, the cubes were removed and washed with a 1x Binding Buffer solution. To release the affinity between Annexin V and the EVs, 10 mM EDTA is added to the device. The chelating agent targets divalent metal ions which removes the necessary calcium ions. Afterward, the isolated sample is squeezed out of the device. The resulting volume absorbed from one ExoSponge ranged from 1.4 ml to 1.9 ml and we further normalized the exosomal concentration using this volume. All samples conjugated with Anti-CD63 protein were washed and prepared with the same procedures but using only filtered PBS instead of binding buffer solution.

***EV isolation/release using ultracentrifugation:*** Ultracentrifugation was used to prepare a exosome model sample and comparison studies. In both cases, a Sorvall ultracentrifuge (ThermoFisher, USA) was used. For comparison study, the same volume of initial plasma/cell culture supernatant sample was used but diluted into equal amount of filtered

buffer solution. Plasma/cell culture supernatant samples were first centrifuged at 2000 g for 15 min, and then 12,000 g for 20 min to remove cellular debris. After initial ultracentrifugation at 100,000 g for 90 min, the supernatant was aspirated, and another 38 mL of PBS was injected for a second round of ultracentrifugation at the same conditions. The pellet after the second UC was gently spiked into buffer solution at the same volume of the ExoSponge resultant solution.

**Scanning electron microscopy (SEM) analysis:** In preparation for SEM imaging, the EV-containing device was treated with 2% glutaraldehyde to retain the morphology, for one hour while on ice. After being rinsed with PBS, the samples were subjected to bath concentrations of ethanol (50%, 70%, 90%, 95%, and 100%) for 10 minutes each (two times for 100%) to dehydrate the samples. Afterwards, hexamethyldisilazane (HMDS) (Emsdium, United States) was used to dry the samples preceding an overnight air drying in the hood. The dehydrated samples were mounted on aluminum stubs using both carbon tape and glue, then sputter-coated with gold particles to form a conductive layer. The TESCAN RISE scanning electron microscope (SEM) at the Michigan Center for Materials Characterization (MC<sup>2</sup>) at the University of Michigan was utilized for the surface imaging.

**EV recovery evaluation using nanoparticle tracking analysis:** After EDTA treatment and sample extraction outlined in section 2.4, the sample is taken to Nanoparticle Tracking Analysis (NTA) using NanoSight NS300 (Malvern Instruments, UK). This process is used to quantify the concentrations and size distribution of our recovered samples from ExoSponge devices. 30  $\mu$ L of the resultant was used and a laser module was mounted inside the main

instrument housing. Based on the Brownian motion of nanoparticles, this equipment visualizes the scattered lights from the particles of interest. This movement was monitored through a video sequence for 20 s in triplicate. All data acquisition and processing were performed using NanoSight NS300 control software. After particle data is recorded based on their size, the area of interest, between 30 and 150 nm, was analyzed for exosomal concentration as well as total vesicle concentration.

***Protein quantity evaluation using Micro-BCA analysis:*** EVs lysates were acquired using RIPA buffer (Cat #: 89900, ThermoFisher Scientific, USA) with 1 % protease inhibitor (Cat#: 78441, ThermoFisher Scientific, USA). The prepared buffer solution was applied to ExoSponge after exosome isolation and washing steps. ExoSponge devices were incubated with RIPA buffer for 10 minutes in a conical tube and followed by mild centrifugation to collect supernatant. Incubated RIPA buffer was collected for micro-bicinchoninic acid (micro-BCA) analysis and incubated with working buffer, as per the manufacturer's instructions, for 2 hours in 37 °C wrapped in aluminum foil. Total protein amount was measured with the Synergy NEO HTS Multi-Mode Reader (Agilent, United States) and by extrapolation through a standard curve generated as per manufacturer's instructions.

***Protein identification using western blot analysis:*** Isolated ExoSponge EV protein lysate was prepared using RIPA buffer (Cat #: 89900, ThermoFisher Scientific, USA) with 1 % protease inhibitor (Cat#: 78441, ThermoFisher Scientific, USA). Sample preparation was conducted by mixing 37.5  $\mu\text{L}$  of ExoSponge lysate with 12.5  $\mu\text{L}$  of Working Buffer (10:1 of Laemmli and 2-mercaptoethanol, respectively) for a 50  $\mu\text{L}$  sample solution. Protein samples

were boiled for 7 minutes, then cooled on ice, and subjected to SDS-PAGE. The proteins were transferred onto polyvinylidene difluoride (PVDF) membranes (Cat#: 1620261, Bio-Rad Laboratories, USA) using a semi-dry Trans-Blot Turbo system (Bio-Rad Laboratories, USA). Blots were incubated in EveryBlot Blocking Buffer (Cat#: 12010020, Bio-Rad Laboratories, USA) for 5 minutes at room temperature and then with their respective primary antibodies (anti-CD63 and anti-GAPDH, Santa Cruz Biotechnology, USA) diluted in TBST (containing 0.1% Sodium azide) overnight at 4 °C. Afterwards, blots were washed with TBST and incubated with anti-rabbit HRP secondary antibodies (Millipore Sigma, USA) in 5% Blotting-Grade Blocker (Cat#: 1706404, Bio-Rad Technologies, USA) and detected using SuperSignal West Pico Chemiluminescent Substrate (Thermo Scientific, USA) and ChemiDoc Imaging System (Bio-Rad Technologies, USA).

***Clinical sample preparation and processing:*** In preparation of ExoSponge isolation, 10 mL of plasma sample was combined with 1 mL of 10x binding buffer solution containing 25 mM of CaCl<sub>2</sub>. (BD Bioscience, USA). Each cube device was placed in a solution volume of 1.5 mL and each one was incubated for 40 minutes at room temperature. For each of the 5 clinical samples, we prepared a group for NTA and micro-BCA analysis. ExoSponge samples going to NTA and protein analysis were subjected to 1 mL of 10mM EDTA treatment with the samples going to BCA and Western Blotting analysis also having a 500 µL solution of 1 mL of RIPA (Radio-Immunoprecipitation Assay) lysis buffer and 10 µL of PIC added. At the same time, equal amounts of sample solution were saved and underwent UC for further performance comparison study.

**Exosomal metabolite extraction for mass spectrometry:** To facilitate metabolite extraction, 750  $\mu$ L of Optima methanol (Cat#: A454-1, ThermoFisher Scientific, USA) at  $-20^{\circ}\text{C}$  and 750  $\mu$ L of Optima water (Cat#: W71, ThermoFisher Scientific, USA) containing 0.5  $\mu\text{g}$  of norvaline internal standard was well mixed with ExoSponge-bound exosomes. The solution was squeezed out from the ExoSponge and centrifuged at 4,000 rpm for 3 minutes to remove debris. The supernatant was combined with an equal volume of chloroform at  $-20^{\circ}\text{C}$  and then vortexed at  $4^{\circ}\text{C}$  for 15 min. The mixed solution was centrifuged at  $17,000\times g$  and  $4^{\circ}\text{C}$  for 10 min to separate into three layers. The upper polar layer of methanol and water containing polar metabolites was pipetted off into a new tube and dried via vacuum centrifugation. The polar metabolites were then resuspended in 50% methanol for LC-MS/MS injection.

**Metabolomics analysis:** The samples are analyzed with SCIEX Triple Quad<sup>TM</sup> 7500 LC-MS/MS QTRAP coupled to ExionLC<sup>TM</sup> system. A scheduled Multiple Reaction Monitoring (MRM) MS method was set up using the following parameters: GS1 = 45 psi, GS2 = 70 psi, spray voltage = 1600 V, Temperature =  $450^{\circ}\text{C}$ , settling time = 15 ms and pause time = 3 ms. The LC method was adapted from a global metabolomics protocol provided by SCIEX. Briefly, analytes were separated using Phenomenex's Kinetex, 2.6  $\mu\text{M}$  F5 100 A (150mm x 2.1mm) equipped with SecurityGuard ULTRA Cartridge. Mobile phase A is 0.1% formic acid in water while mobile phase B is 0.1% formic acid in acetonitrile. Analysis time is 20 min with the following gradient: 0 min 0% B, 2.1 min 0% B, 14 min 95% B, 16 min 95% B, 16.1 min 0% B and finally 20 min 0% B. Column temperature was set at  $30^{\circ}\text{C}$ . The flowrate is 0.2 mL/min and 1-5  $\mu$ L of each sample was injected per run. Peaks were extracted and integrated by SCIEX OS 2.0, after filtering for good quality peaks. Peak quality was estimated by SCIEX OS based on peak height, width at half-height, signal-to-noise ratio and

retention time shift. Finally, software-assigned good quality peaks were checked visually and filtered further. Peak areas of all metabolites were normalized to the volume of plasma used to isolate exosomes and the peak area for the internal standard, Norvaline. Further, analysis was performed with MetaboAnalyst 5.0. One-factor statistical analysis was used for estimating fold-change and multiple hypotheses testing. Enrichment analysis was used to identify metabolite-associated disease signatures from the blood and urine biomarker sets available in the MetaboAnalyst 5.0 knowledgebase.

**Statistical Analysis:** All results present as mean  $\pm$  standard deviation. Statistical analysis were demonstrated using Prism software. Unpaired t-tests (two-tailed) were used to compare the differences of exosome-sized vesicles concentration between lung cancer patients (n = 6) versus healthy controls (n = 4). Statistical significance was defined as a two-tailed  $p < 0.05$ . For metabolomics analysis, One-factor statistical analysis was used for estimating fold-change and multiple hypotheses testing.

### Supporting Information

Supporting Information is available from the Wiley Online Library or from the author.

### Acknowledgements:

The authors thank Thomas Hadlock for initial help in porous PDMS procedure. The authors also acknowledge the Lurie Nanofabrication Facility at the University of Michigan. The authors acknowledge the financial support of the University of Michigan College of Engineering and NSF grant #DMR-0320740, and technical support from the Michigan Center for Materials Characterization. Dr. Yoon-Tae Kang is an Innovation Fellow supported by Biointerfaces Institute, University of Michigan. This work was also supported by grants from National Institute of Health (NIH), 5-R33-CA-202867-02 to S.N. and 1-R01-CA-208335-01-A1 to S.N.

**Disclosure of Interests:** The authors declare no competing financial interests.

**Data availability**

The authors declare that all data supporting the findings of this study are available within the paper and its Supplementary Information. The raw and analyzed datasets generated during the study are available for research purposes from the corresponding authors upon reasonable request.

Received: ((will be filled in by the editorial staff))

Revised: ((will be filled in by the editorial staff))

Published online: ((will be filled in by the editorial staff))

**References**

- [1] Simons, M. & Raposo, G., Exosomes-vesicular carriers for intercellular communication. *Curr. Opin. Cell. Biol.* 21, 575-581 (2009).
- [2] Whiteside, T.L. Tumor-derived exosomes and their role in cancer progression. *Adv. Clin. Chem.* 74, 103-141 (2016).
- [3] Lane, R. E., Korbie, D., Hill, M. M. & Trau, M. Extracellular vesicles as circulating cancer biomarkers: opportunities and challenges. *Clin. Transl. Med.* 7, 14 (2018).
- [4] Hanahan, D. & Weinberg, R.A. Hallmarks of Cancer: The Next Generation. *Cell* 144, 646-674 (2011).
- [5] Ludwig, N., Whiteside, T. L. & Reichert, T. E. Challenges in Exosome Isolation and Analysis in Health and Disease. *Int. J. Mol. Sci.*, 20, 4684 (2019)
- [6] Niu, Z., Pang, R.T.K., Liu, W., Li, Q., Cheng, R. & Yeung, W.S.B. Polymer-based precipitation preserves biological activities of extracellular vesicles from an endometrial cell line. *PLoS One* 12, e0186534 (2017).
- [7] Multia, E., Tear, C. J. Y., Palviainen, M., Siljander, P., & Riekkola, M. L. (2019). Fast isolation of highly specific population of platelet-derived extracellular vesicles from blood plasma by affinity monolithic column, immobilized with anti-human CD61 antibody. *Analytica Chimica Acta*, 1091, 160-168.
- [8] Multia, E., Liangsupree, T., Jussila, M., Ruiz-Jimenez, J., Kemell, M., & Riekkola, M. L. (2020). Automated on-line isolation and fractionation system for nanosized biomacromolecules from human plasma. *Analytical Chemistry*, 92(19), 13058-13065.
- [9] Zhang, P., He, M. & Zeng, Y. Ultrasensitive microfluidic analysis of circulating exosomes using a nanostructured graphene oxide/polydopamine coating. *Lab chip*, 16, 3033-3042 (2016)

- [10] Kang, Y.-T., Kim, Y.J., Bu, J., Cho, Y.-H., Han, S.-W. & Moon, B.-I. High-purity capture and release of circulating exosomes using an exosome-specific dual-patterned immunofiltration (ExoDIF) device. *Nanoscale*, 9, 13495-13505 (2017)
- [11] Lee, K., Shao, H., Weissleder, R. & Lee, H. Acoustic Purification of Extracellular Microvesicles. *ACS Nano*, 9, 2321-2327 (2015)
- [12] Liu, F. et al. The exosome total isolation chip. *ACS Nano*, 11, 10712-10723 (2017)
- [13] Kang, Y.-T., Kim, Y.J., Rupp, B., Purcell, E., Hadlock, T., Ramnath, N. & Nagrath, S., Isolation of Circulating Biomarkers for Liquid Biopsy using Immunoaffinity-Based Stimuli-Responsive Hybrid Hydrogel Beads. *Anal. Sens.* 1, 117-129 (2021)
- [14] Raj M., K. & Chakraborty, S. PDMS microfluidics: A mini review. *J. Appl. Polym. Sci.* 137, 48958 (2020).
- [15] Fujii, T. PDMS-based microfluidic devices for biomedical applications. *Microelectron. Eng.* 61-62, 907-914 (2002).
- [16] Takeuchi, K., Takama, N., Kinoshita, R., Okitsu, T. & Kim, B. Flexible and porous microneedles of PDMS for continuous glucose monitoring. *Biomed. Microdevices.* 22, 79 (2020).
- [17] Li, Q., Duan, T., Shao, J. & Yu, H. Fabrication method for structured porous polydimethylsiloxane (PDMS). *J. Mat. Sci.* 53, 11873-11882 (2018).
- [18] Masihi, S., et al. Highly Sensitive Porous PDMS-Based Capacitive Pressure Sensors Fabricated on Fabric Platform for Wearable Applications. *ACS Sens.* 6, 938-949 (2021).
- [19] Yu, C., Yu, C., Cui, L., Song, Z., Zhao, X., Ma, Y. & Jiang, L. Facile Preparation of the Porous PDMS Oil-Absorbent for Oil/Water Separation. *Adv. Mat. Interfaces.* 4, 1600862 (2016)
- [20] Norfatriah, A., Syamaizar, A.S.A & Zuruza, A.S. Application of Porous Polydimethylsiloxane (PDMS) in oil absorption, *IOP Conf. Ser.: Mater. Sci. Eng.* 342, 012050 (2018).
- [21] Yoon S, Seok M, Kim M, Cho YH. Wearable porous PDMS layer of high moisture permeability for skin trouble reduction. *Sci Rep.* 2021 Jan 13;11(1):938.
- [22] M.G. King, A.J. Baragwanath, M.C. Rosamond, D. Wood, A.J. Gallant, Porous PDMS force sensitive resistors, *Procedia Chemistry*, Volume 1, Issue 1, 2009, 568-571
- [23] Suthar J. et al Acoustic Immunosensing of Exosomes Using a Quartz Crystal Microbalance with Dissipation Monitoring *Anal. Chem.* 2020, 92, 5, 4082–4093
- [24] Kang YT, Purcell E, Palacios-Rolston C, Lo TW, Ramnath N, Jolly S, Nagrath S. Isolation and Profiling of Circulating Tumor-Associated Exosomes Using Extracellular



Vesicular Lipid-Protein Binding Affinity Based Microfluidic Device. *Small*. 2019 Nov;15(47):e1903600.

[25] Achreja, A., Meurs, N. & Nagrath, D. Quantifying Metabolic Transfer Mediated by Extracellular Vesicles Using Exo-MFA: An Integrated Empirical and Computational Platform. *Metabolic Flux Analysis in Eukaryotic Cells*, 2088, 205-221 (2020).

[26] Zhao, H., et al. Tumor microenvironment derived exosomes pleiotropically modulate cancer cell metabolism. *Elife*. 5, e10250 (2016).

[27] Kumar, S.R., Kimchi, E.T., Manjunath, Y., Gajagowni, S., Stuckel, A.J. & Kaifi, J.T. RNA cargos in extracellular vesicles derived from blood serum in pancreas associated conditions. *Sci. Rep.* 10, 2800 (2020).

[28] Achreja, A., Zhao, H., Yang, L., Yun, T.H., Marini, J., & Nagrath, D. Exo-MFA - A 13C metabolic flux analysis framework to dissect tumor microenvironment-secreted exosome contributions towards cancer cell metabolism. *Matab. Eng.* 43, 156-172 (2017).

[29] Zhao, H., Achreja, A., Lessi, E., Logozzi, M., Mizzoni, D., Raimo, R.D., Nagrath, D. & Fais, S. The key role of extracellular vesicles in the metastatic process. *Biochim. Biophys. Acta. Rev. Cancer*, 1869, 64-77 (2018).

[30] Du, Y., Chen, L., Li, X.-S., Li, X.-L., Xu, X.-D., Tai, S.-B., Yang, G.-L., Tang, Q., Liu, H., Liu, S.-H., Zhang, S.-Y. & Cheng, Y. Metabolomic Identification of Exosome-Derived Biomarkers for Schizophrenia: A Large Multicenter Study. *Schizophr. Bull.* 47, 615-623 (2021).

[31] Tao, L., Zhou, J., Yuan, C., Zhang, L., Li, D., Si, D., Xiu, D. & Zhong, L. Metabolomics identifies serum and exosomes metabolite markers of pancreatic cancer. *Metabolomics*. 15, 86 (2019)

[32] Zebrowska, A., Skowronek, A., Wojakowska, A., Widlak, P. & Pietrowska, M. Metabolome of Exosomes: Focus on Vesicles Released by Cancer Cells and Present in Human Body Fluids. *Int. J. Mol. Sci.* 20. 3461 (2019).

[33] Zhang, L., Li, Q., Yang, R., Xu, Z., Kang, Y & Xue, P. Rapid prototyping of Nanoroughened polydimethylsiloxane surfaces for the enhancement of immunomagnetic isolation and recovery of rare tumor cells. *Biomed. Microdevices*. 21, 58 (2019)

[34] Chen, W., Weng, S., Zhang, F., Allen, S., Li, X., Bao, L., Lam, R.H.W., Macoska, J.A., Merajver, S.D. & Fu, J. Nanoroughened Surfaces for Efficient Capture of Circulating Tumor Cells without Using Capture Antibodies. *ACS Nano*. 7, 566-575 (2013)

[35] Mokhtarani, M. et al. Urinary phenylacetylglutamine as dosing biomarker for patients with urea cycle disorders. *Mol. Genet. Metab.* 107, 308-314 (2012)

- [36] Machado, M.C.C. & Silva, F.P. Hyperammonemia due to urea cycle disorders: a potentially fatal condition in the intensive care setting. *J. Intensive Care.* 2, 22 (2014)
- [37] Nemet, I. et al. A Cardiovascular Disease-Linked Gut Microbial Metabolite Acts via Adrenergic Receptors. *Cell.* 180, 862-877 (2020).
- [38] Reichard, C.A., Naelitz, B.D., Wang, Z., Jia, X., Li, J., Stampfer, M.J., Klein, E.A., Hazen, S.L. & Sharifi, N., Gut Microbiome-Dependent Metabolic Pathways and Risk of Lethal Prostate Cancer: Prospective Analysis of a PLCO Cancer Screening Trial Cohort. *Cancer Epidemiol. Biomarkers Prev.* 31, 192-199 (2022).
- [39] Lee, J.S. et al. Urea Cycle Dysregulation Generates Clinically Relevant Genomic and Biochemical Signatures. *Cell.* 174, 1559-1570 (2018).
- [40] Gomes, A.P. et al. Age-induced accumulation of methylmalonic acid promotes tumour progression. *Nature.* 585, 283-287 (2020).
- [41] Amjadi, M., Kim, M.S. & Park, I. Flexible and sensitive foot pad for sole distributed force detection. *IEEE 14th international conference on nanotechnology (IEEE-NANO)*, IEEE, pp 764–767 (2014)
- [42] Lo, L.-W., Zhao, J., Wan, H., Wang, Y., Chakrabartty, S. & Wang, C. A Soft Sponge Sensor for Multimodal Sensing and Distinguishing of Pressure, Strain, and Temperature. *ACS Appl. Mat. Interfaces.* 14, 9570-9578 (2022).
- [43] Kim, Y.J., Kang, Y.-T. & Cho, Y.-H. Poly(ethylene glycol)-Modified Tapered-Slit Membrane Filter for Efficient Release of Captured Viable Circulating Tumor Cells. *Anal. Chem.* 88, 7938-7945 (2016).
- [44] Zhang, L., Li, Q., Yang, R., Xu, Z., Kang, Y & Xue, P. Rapid prototyping of Nanoroughened polydimethylsiloxane surfaces for the enhancement of immunomagnetic isolation and recovery of rare tumor cells. *Biomed. Microdevices.* 21, 58 (2019)
- [45] Chen, W., Weng, S., Zhang, F., Allen, S., Li, X., Bao, L., Lam, R.H.W., Macoska, J.A., Merajver, S.D. & Fu, J. Nanoroughened Surfaces for Efficient Capture of Circulating Tumor Cells without Using Capture Antibodies. *ACS Nano.* 7, 566-575 (2013)

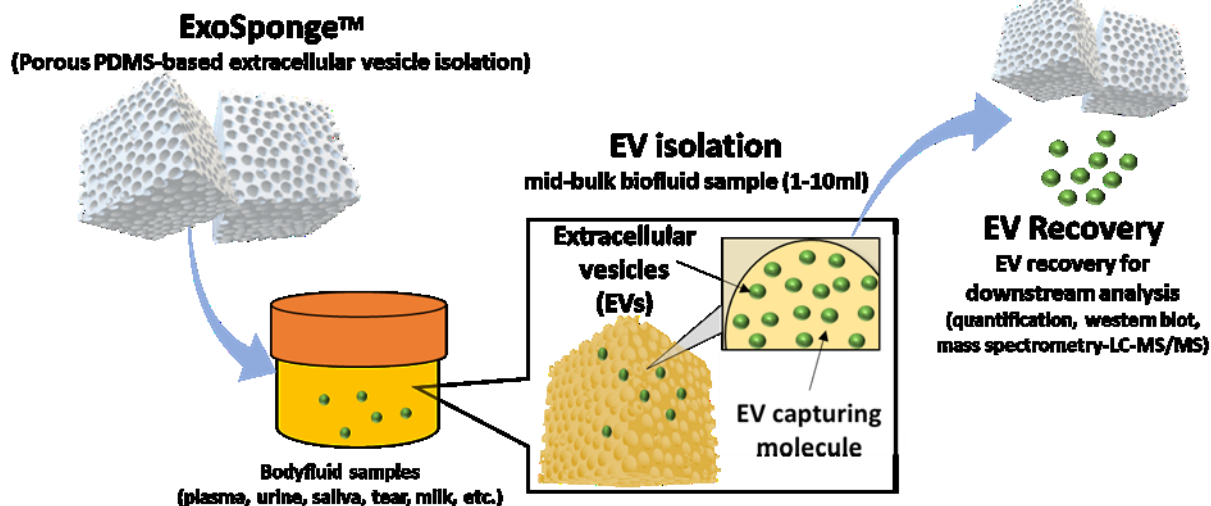
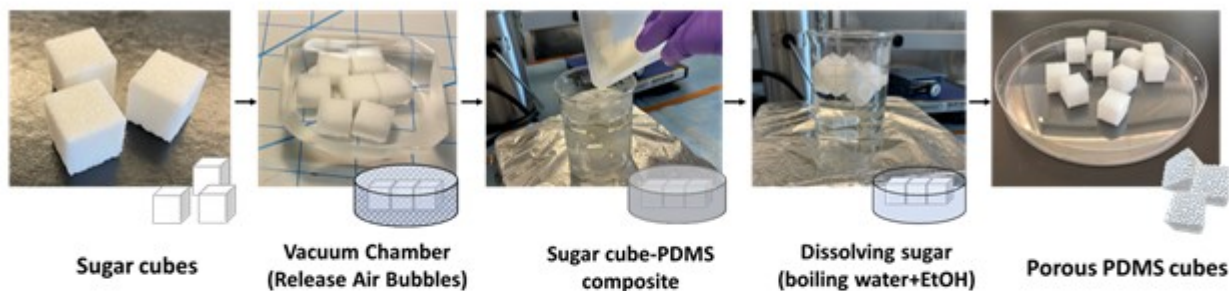


**Figure 1.** Porous polydimethylsiloxane (PDMS) based cancer-associated extracellular vesicle isolation and recovery from body fluid samples

#### a. Porous PDMS fabrication



#### b. Surface modification of Porous PDMS

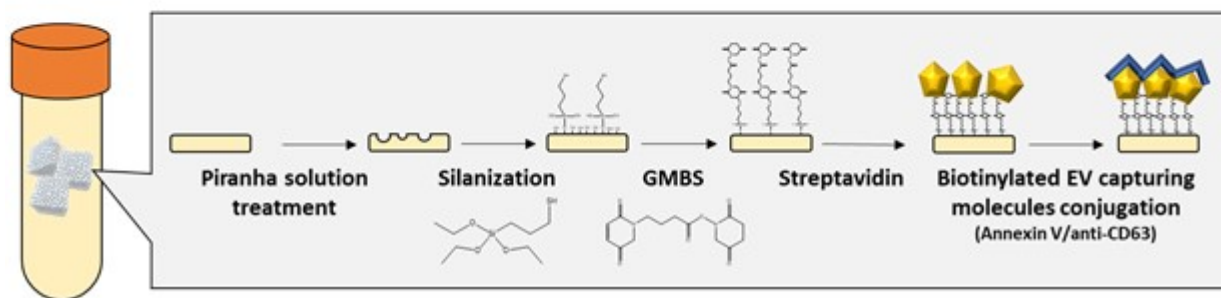


**Figure 2.** Fabrication and surface modification of porous PDMS cubes to isolate circulating biomarkers: (a) Porous PDMS unit device created using sugar cube scaffold; Sugar cubes were submerged in PDMS solutions and then PDMS adsorbed sugar cubes were cured. Then the sugar is dissolved to reveal the porous PDMS 3-D structures. (b) surface modification of porous PDMS unit to isolate circulating biomarkers.

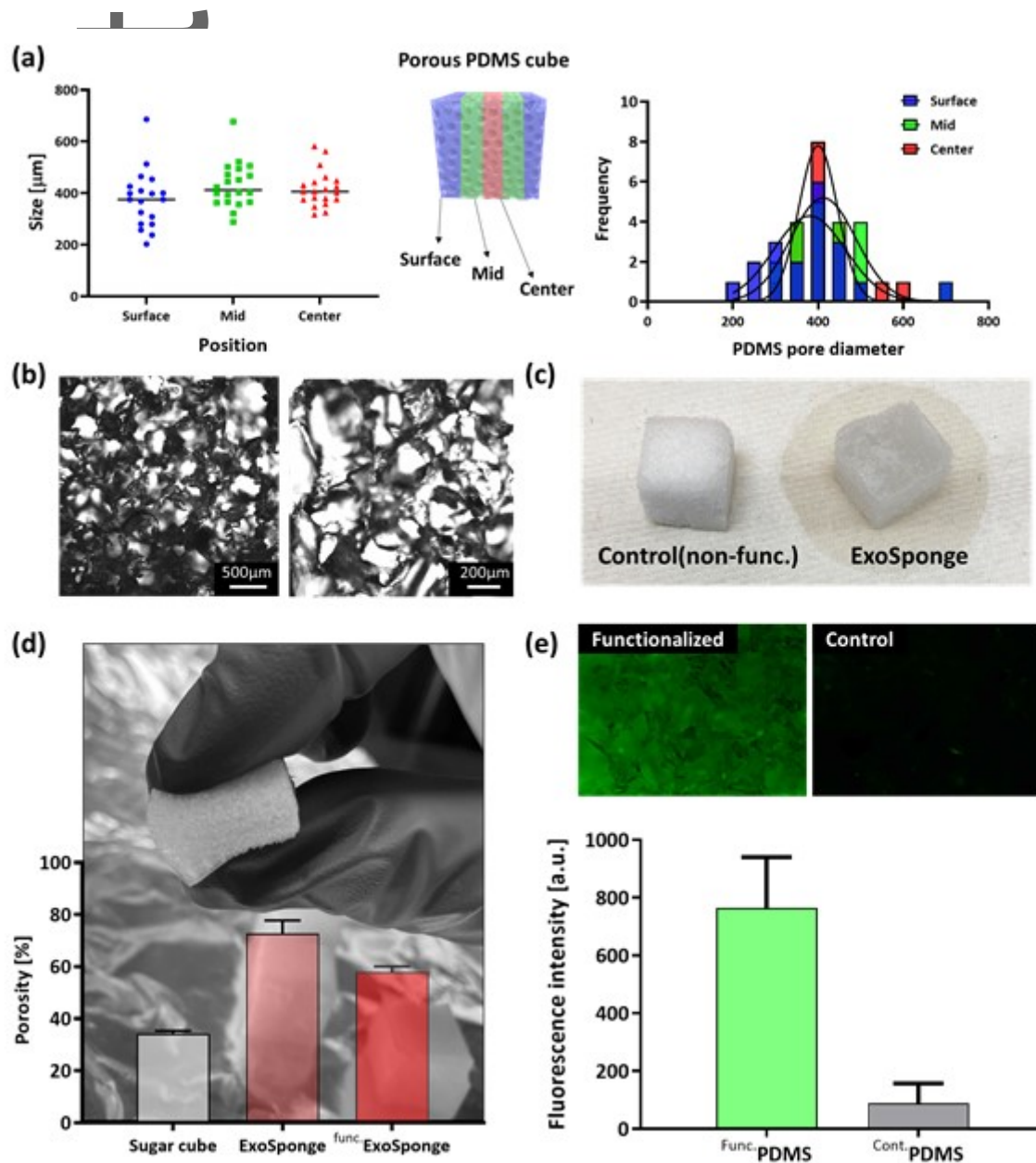


**Figure 3.** Evaluation of porous PDMS fabrication and functionalization: **(a)** pore size evaluation at surface, mid-center, and center (left), and pore size distribution at the three different locations (right); **(b)** microscopic images of porous PDMS cube slices; **(c)** evaluation of wettability in porous PDMS unit between pre-functionalization (hydrophobic) and post-functionalization (hydrophilic); **(d)** porosity evaluation for sugar cube, porous PDMS unit and functionalized porous PDMS unit, ExoSponge; **(e)** quantitative analysis of fluorescence intensities between avidin-functionalized device and control device after biotinylated fluorescence dye (top left) and its surface under fluorescence microscopy (top right)

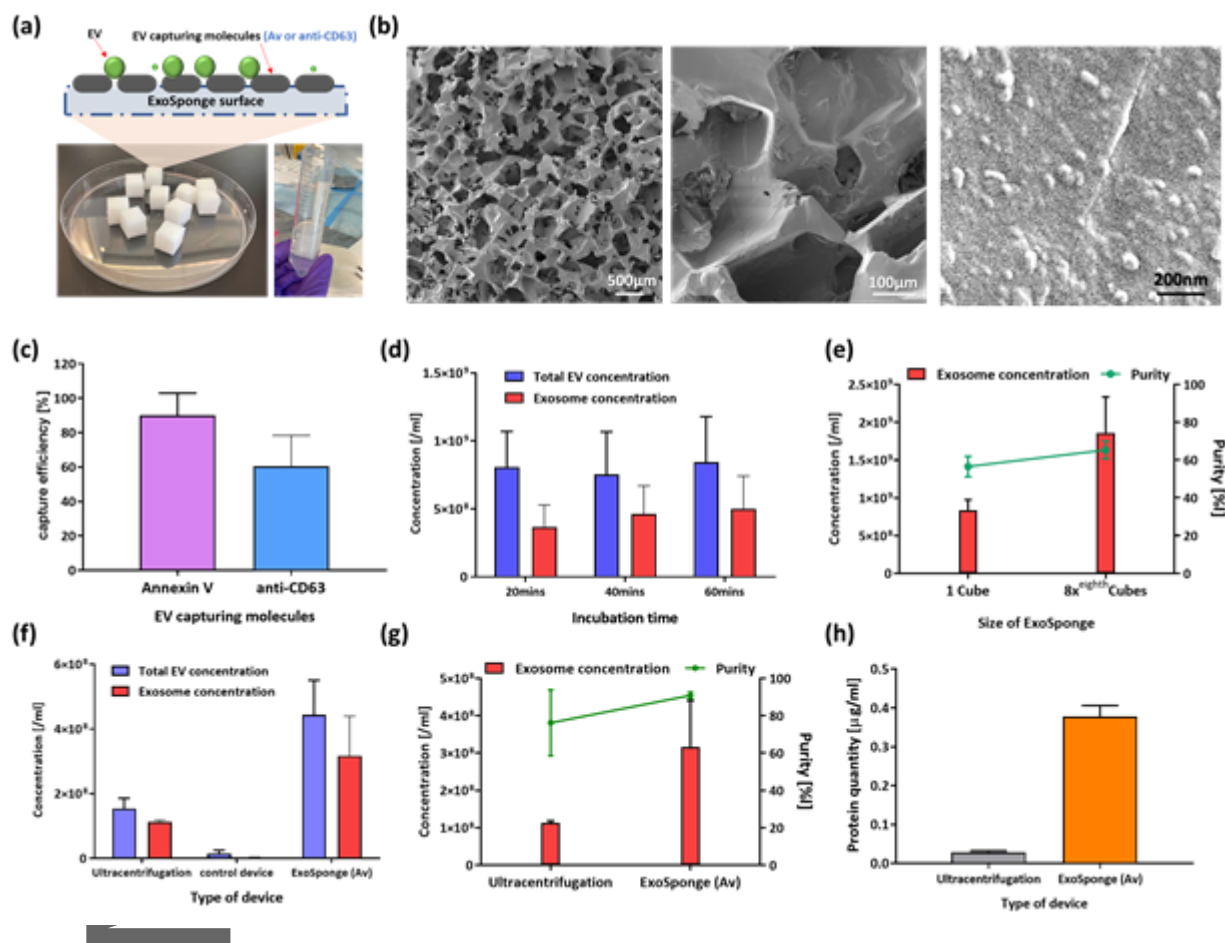


**Figure 4.** Cancer-associated extracellular vesicle (EV) isolation using porous PDMS cubes (ExoSponge) via Annexin V conjugation onto the device: **(a)** fabricated and functionalized ExoSponge unit devices and working principle of extracellular vesicle isolation; **(b)** scanning electron microscope microscopy analysis of ExoSponge undergone EV isolation; **(c)** EV capturing performance of ExoSponge conjugated with Annexin V (Av) or anti-CD63; **(d)** EV isolation performance depending incubation time with samples; **(e)** exosome concentration comparison between 1 unit device and 8x 1/8unit devices; **(f-h)** EV isolation comparison study with gold-standard extracellular vesicle isolation, ultracentrifugation, in terms of EV concentration (f), purity and exosome concentration (g), and total protein quantity (h).



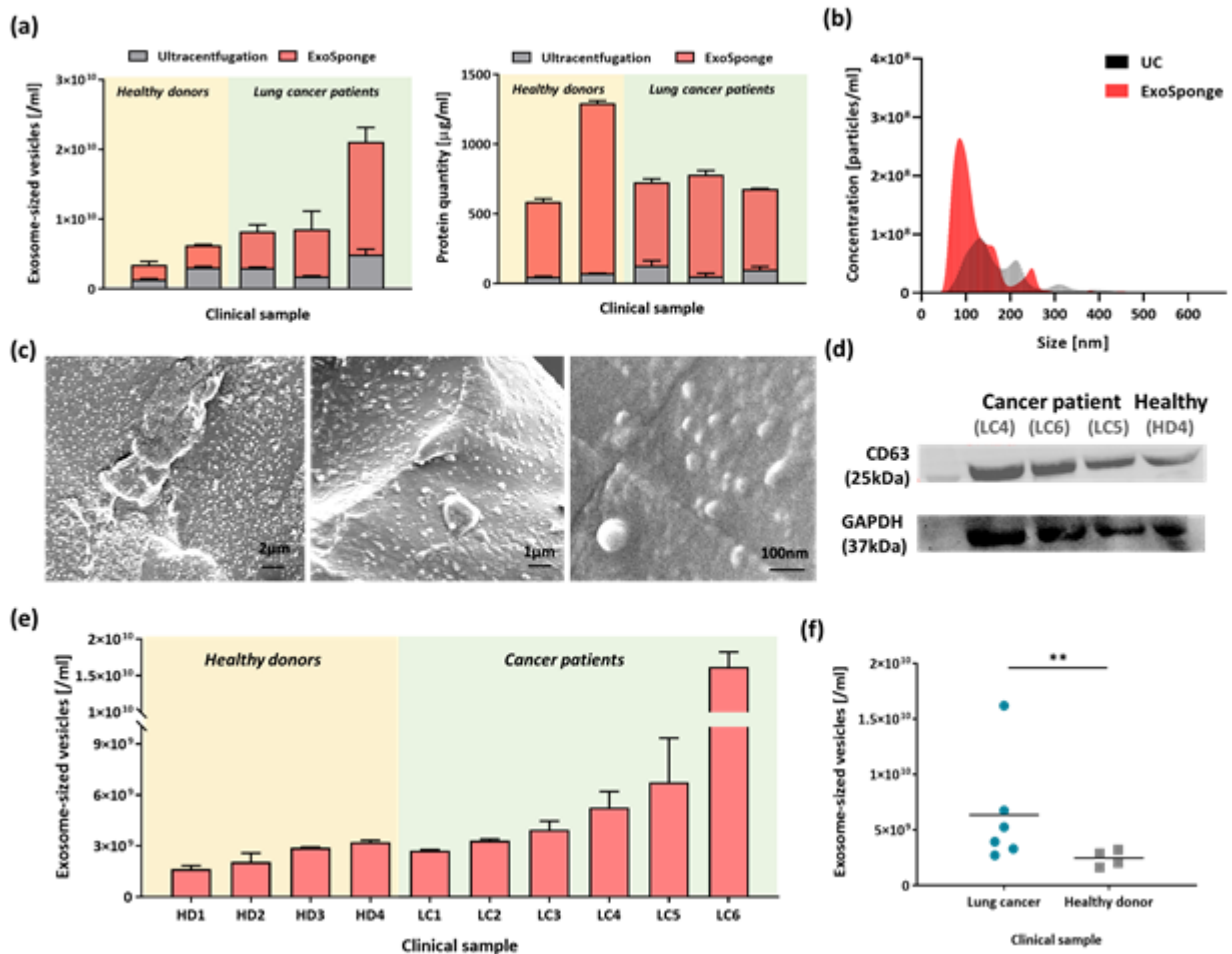


**Figure 5.** Clinical utility of ExoSponge (Av) platform in recovering intact extracellular vesicles (EVs) and analyzing EVs for quantitative/qualitative studies: **(a)** EV isolation performance comparison in terms of exosome-sized vesicle concentration (left) and total protein quantity (right); **(b)** nanoparticle tracking analysis of resultants from ExoSponge and UC; **(c)** scanning electron microscopic analysis of isolated EVs on ExoSponge platform; **(d)** western blot analysis of ExoSponge resultant samples; **(e)** exosome isolation from healthy donors and cancer patients using ExoSponge; **(f)** exosome-sized vesicle concentration comparison between two groups (line at mean value).

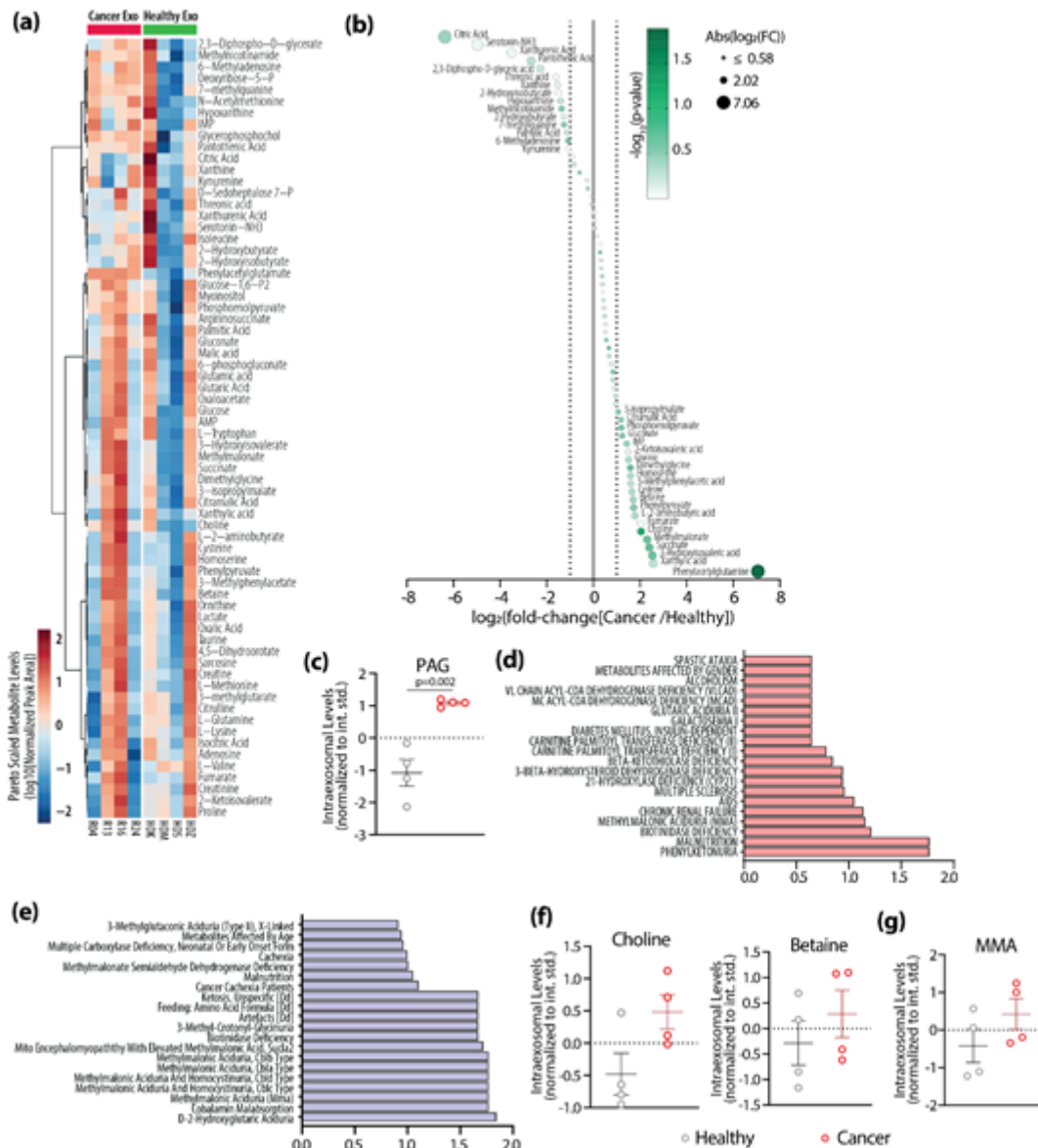


**Figure 6.** Analysis of exosomal metabolites isolated using ExoSponge conjugated with Annexin V: **(a)** Heatmap of intraexosomal metabolite levels detected by LC-MS/MS in cancer-derived exosomes (Red) compared to exosomes from healthy subjects (Green); **(b)** Waterfall plot demonstrating differentially abundant intraexosomal metabolites from cancer patient-derived samples compared to healthy subjects; **(c)** Intraexosomal metabolite level of phenylacetylglutamine; **(d)** MSEA showing top 20 metabolite sets representing disease signatures in plasma metabolites, enriched in exosomes from cancer patients compared to healthy subjects; **(e)** MSEA showing top 20 metabolite sets representing disease signatures in urine metabolites, enriched in exosomes from cancer patients compared to healthy subjects; **(f)** Intraexosomal metabolite level of betaine and choline; **(g)** Intraexosomal metabolite level of methylmalonate. Metabolite levels were analyzed using MetaboAnalyst 5.0 after normalizing metabolite signals to sample-specific internal standard, mean-centered and Pareto-scaled.

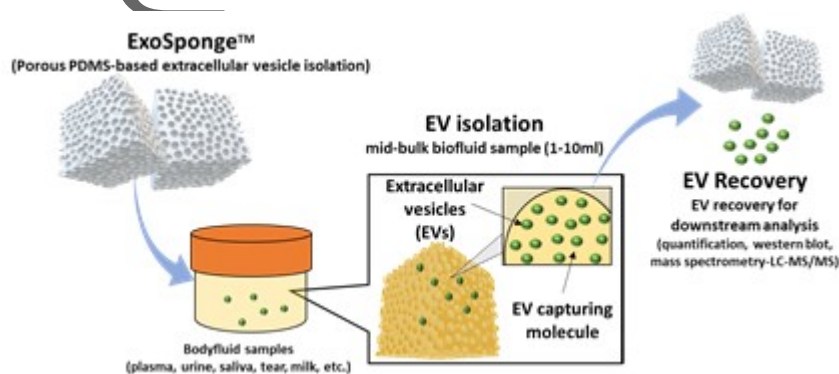
DOI: 10.1002/((please add manuscript number))

## Table of Contents

**Keyword:** Porous PDMS-based EV isolation for liquid biopsy

Joseph Marvar<sup>1,+</sup>, Abha Kumari<sup>1,+</sup>, Nna-Emeka Onukwughu<sup>1</sup>, Abhinav Achreja<sup>2</sup>, Noah Meurs<sup>2</sup>,  
Olamide Animasahun<sup>2</sup>, Jyotirmoy Roy<sup>2</sup>, Miya Paserba<sup>2</sup>, Kruthi Srinivasa Raju<sup>1</sup>, Shawn Fortna<sup>3</sup>,  
Nithya Ramnath<sup>4</sup>, Deepak Nagrath<sup>1,2</sup>, Yoon-Tae Kang<sup>1,\*</sup>, and Sunitha Nagrath<sup>1,5\*</sup>

## Porous PDMS-based Microsystem (ExoSponge) for Rapid Cost-effective Tumor Extracellular Vesicle Isolation and Mass Spectrometry-based Metabolic Biomarker Screening



Analysis of extracellular vesicles (EVs) as biomarkers in liquid biopsy systems have been a promising avenue in disease detection. While there are many technologies developed for the isolation of EVs, their procedures typically require expensive machinery or are limited by their low throughput. The porous PDMS-based microsystem, ExoSponge, introduces a scalable, cost-effective platform for EV isolation and metabolic biomarker screening.